Parametric Study of Parachute Pressure Distribution by Wind Tunnel Testing

W. B. Pepper* and J. F. Reed*
Sandia Laboratories, Albuquerque, N. Mex.

Pressure distribution data for solid and ribbon parachutes are presented. Three-foot diameter model parachutes of 0, 10, 15, 20, 25, 30, and 40% geometric porosity were tested. Suspension line lengths of 1.0, 1.5, and 2.0 constructed diameters were used. Reefing line lengths of 19, 38, and 57 in. were tested. Two 7 x 10 ft wind tunnels were used to test over a range of dynamic pressures from 35 to 600 lb/ft^2.

Integration of the measured pressures over the inflated canopy profiles generally resulted in drag force values which agree within 10% of force balance drag data.

Nomenclature

C_{D_o} = drag coefficient based on constructed area, $D/(qS_o)$
$C_{D\Delta p}$ = integrated pressure drag coefficient (D_{ACTUAL}/qS_o)
D = drag, lb.
D_i = inflated diameter (in.)
D_o = constructed parachute diameter, 36 in.
D_p = inflated parachute diameter as measured from 70-mm photos, in.
D_{ACTUAL} = Final value of pressure drag including compensation of chute porosity, $D_{ACTUAL} = D_{TOTAL}$ (1.00% porosity/100), lb
D_{TOTAL} = drag as integrated from pressure taps, lb
FXX = parachute model with XX indicating percent geometric porosity
LXX = shroud line length with XX indicating shroud line length in constructed chute diameters
L/D_o = ratio of shroud line length to constructed diameter
L/R = ratio of distance from center of chute vent to pressure port, to the distance from center of vent to skirt, with all distances measured along chute surface
P = pressure, psf or indication of pressure chute configuration in run description
Q,q = freestream dynamic pressure, psf
Rxx,L_r = reefing line length, with XX indicating length in inches
S_o = reference area based on constructed diameter (D_o), ft^2
t = time from initiation of disreefing, sec
V_∞ = freestream velocity, fps
α = angle between centerline of inflated chute and normal to chute surface at a pressure port location, deg.
λ = geometric porosity, percent of S_0

Received Oct. 17, 1975: presented as Paper 75-1369 at the AIAA 5th Aerodynamic Deceleration Systems Conference, Albuquerque, N. Mex., Nov 17-19, 1975: revision received June 10, 1976. Appreciation is given to the following personnel for assisting with this project: R. T. McVeety, 5623, for test hardware design; D.A. Powers, 5645, for handling dynamic pressure measurement instrumentation; J.W. Holbrook and J.B. Vaughn, Vought Systems Division, LTV; Aerospace Corporation, Grand Prairie, Tex., for conducting wind tunnel tests at LTV; J. Ottensoser, Naval Ship Research and Development Center, Bethesda, Md., for conducting wind tunnel tests and for analysis of data at NSRDC. This work was supported by the United States Energy Research and Development Administration.

Index categories: Aircraft Deceleration Systems; Entry Deceleration Systems and Flight Mechanics (e.g., Parachutes).

*Member of Technical Staff, Aerodynamics Department 1330. Associate Fellow AIAA.

Introduction

IN order to analyze parachute stresses on any recovery system, it is necessary to have the dynamic history of pressure distribution over the canopy and the canopy profile. In 1959[1] Sandia Laboratories first made static pressure measurements on a 34.4 in. diameter ribbon parachute in a wind tunnel. The tests were conducted over a dynamic pressure range of 100 to 400 lb/ft^2. Only one configuration, of approximately 25% geometric porosity, with one suspension line length was tested. The side view profiles which are necessary for stress analysis were not documented in Ref. 1 and are no longer available.

Heinrich[2,3] has contributed greatly to the field of pressure measurement. In Ref. 2 he analyzed pressure measurements made by Melzig[4] on solid flat and ring slot canopies, finding large discrepancies between the integrated pressure drag and force measurements.

Due to the lack of pressure data, a thorough parametric study was undertaken by Sandia Laboratories. This report discribes the results of pressure distribution measurements[5-7] on 3 ft diameter ribbon parachutes. The force measurements taken during these same wind tunnel tests are presented by McVey[8].

Model Parachutes

The nylon parachutes† (Fig. 1) had 24 gores and were 3 ft nominal diameter across the base of the 20 deg conical construction cone. The vent diameter was 10%, or 3.6 in. Suspension line length was *2 D_o* (72 in.) with loops at *1.5 D_o* and *1.0 D_o*. Suspension lines of 220 lb tensile strength were continous over the canopy. The 3/8 in. wide horizontal ribbons were of 58 lb tensile strength. Five 40 lb cord verticals per gore were used. A complete description of the materials used is given in Table 1. Geometric porosities of 0, 10, 15, 20, 25, 30, and 40% were tested. Reefing rings (1/4 in. I.D. split rings used in fishing tackle) were sewn to the skirt band at each intersection with the 24 suspension lines.

The static pressure instrumentation consisted of two flexible clear plastic strip tubes (1/16 in. O.D. $\times$ 1/32 in. I.D.) glued and tied to each radial alternating inside and outside of the canopy and extending out aft of the vent. Notches were cut in the tubes at 23 radial stations both on the inside and the outside of the canopy.

Test Procedure and Instrumentation

The first test series was conducted in the LTV Vought Systems Division 7 x 10 ft Low Speed Wind Tunnel, Grand

†All parachutes were manufactured by ILC Steinthal, Inc., Roxboro, N.C.

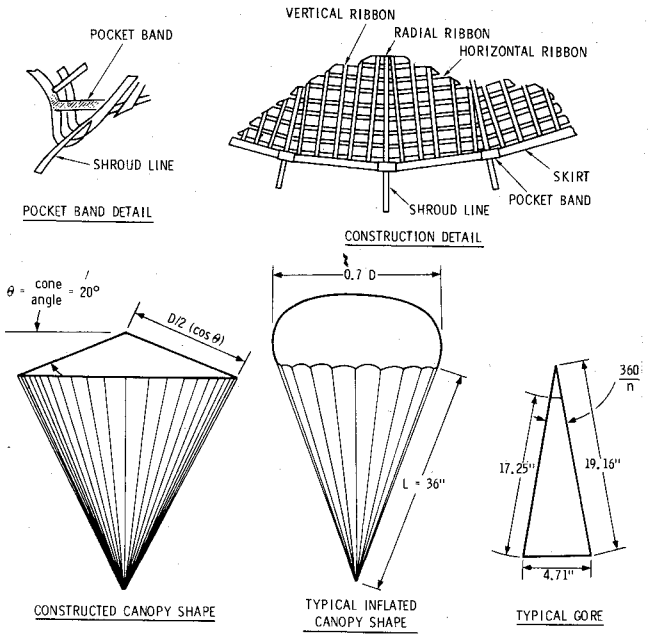

Fig. 1 Model dimensional data.

Prairie, Tex. A schematic of the model setup can be seen as Fig. 2. The 46 flexible tubes were taped loosely to the guide rod and were allowed to slide freely on the rod downstream of the canopy as shown in Fig. 3.This technique permitted relatively interference-free measurement of parachute drag through the use of a one-component strain-gage balance located in the cable-supported ogive-cylinder model. The flexible pressure tubing terminated in a scanivalve and pressure transducer which scanned the 46 ports to record the pressure data. The locations to the ports are given in Table 2. Side view photographs (see Fig. 7 for a typical example) were taken of each configuration to determine canopy profile shape. The profiles from the pressure models and force models, which have no pressure tubing, are coincident.

The second series was also conducted at LTV using only the 25% geometric porosity ribbon parachute shown in Fig. 4. The purpose of the program was to measure the canopy differential pressure distribution during dynamic inflation after disreefing. For these tests, seven Kulite differential pressure transducers‡ were sewn to the inside of the canopy at seven radial stations as shown in Fig. 5. These gages were 0.625 x 1.25 0.1 and had a range of −1 to +3 psid.

The third test series was conducted at the Naval Ship Research and Development Center, Bethesda, Md., using their 7 x 10 ft transonic tunnel. This program was designed to determine the effects of dynamic pressure variation (from 75 to 600 psi) and Mach number (from 0.225 to 0.780). Most of the data presented herein are from the NSRDC program. The tunnel installation and instrumentation were the same as in the LTV wind tunnel. The same parachutes were utilized. The dynamic opening pressure distribution tests were not repeated at NSRDC.

‡Pressure tranducers (model no. LQ-38-125-3D) were developed by Kulite Semiconductor Products, 1030 Hoyt Av., Ridgefield, N.J., to Sandia Laboratories specifications.

Table 1 Nylon materials used for construction of 3-ft-diameter ribbon parachute models

Component	USAF Mil Spec	Type	Width (in)	Tensile Strength (lb)
Suspension Lines	C-5040	III[a]	1/8	220
Horizontal Ribbons	T-5608	II	3/8	58
Verticals	C-5040	I[a]	1/16	40
Skirt and Vent Bands	T-5038	III	3/8	200
Reefing Lines				
Thread	T-7807B	I	1/32 dia.	40
Cord (double)	C-5040B	I	1/16 dia.	100

Test	Cutter Type	Dia. (in)	Length (in)	Max Cord Strength Will Cut (lb)
LTV	Atlas[b]	0.185	0.75	100
NSRDC	Tech Ordnance[c]	0.320	2.0	750

[a] Casing only.
[b] Model No. 1 SE 192.
[c] Model No. 1 SE 166.

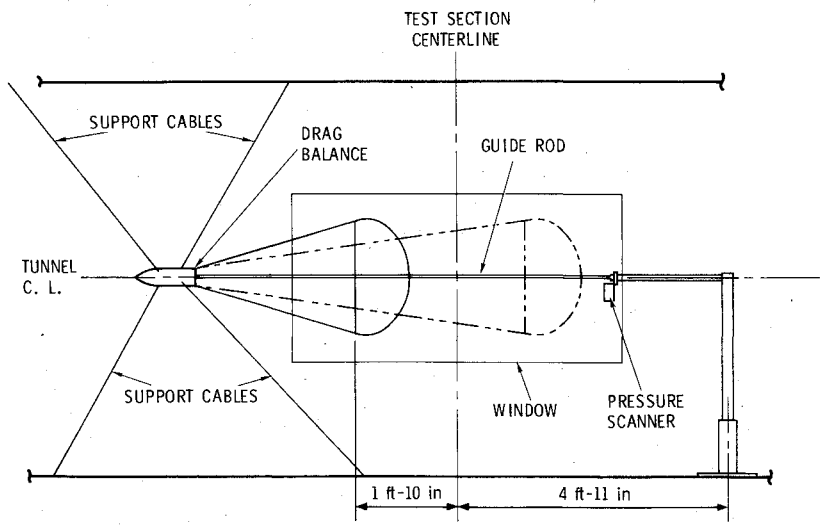

Fig. 2 Schematic of model setup.

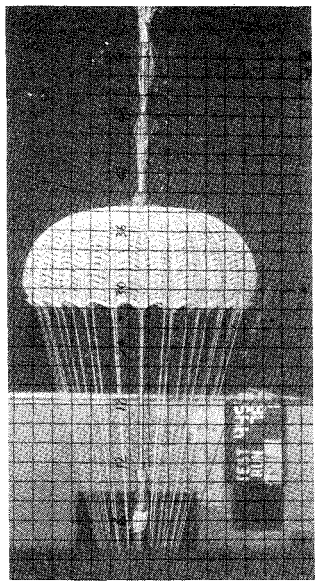

Fig. 3 Parachute installation sketch.

Data Reduction

Pressures from the 23 ports on the inside of the canopy and from the 23 ports on the outside of the canopy were fed to separate scanivalves which were gauged to read the same port number of each scanivalve simultaneously, These taps surveyed the inside and the outside pressure distribution from vent to skirt.

In order to attempt to verify the accuracy of the data, the pressures were integrated to yield drag force. The following assumptions and steps were taken to integrate for drag:

$$D=\int_o^{\ell} P2\pi\cos\alpha y\,ds \tag{1}$$

Cos $\alpha = dy/ds$ and since y is double valued from y_b to y_c,

$$D=\int_{y_a}^{y_b} P2\pi y\,dy+\int_{y_b}^{y_c} P2\pi y\,dy \tag{2}$$

Table 2 Pressure orifice location

Distance from vent center (in)	Outside orifice number	Inside orifice number	Orifice location ratio L/R
16.80	1	25	.917
16.12	2	26	.879
15.44	3	27	.841
14.71	4	28	.803
14.08	5	29	.766
13.39	6	30	.727
12.71	7	31	.689
12.03	8	32	.652
11.35	9	33	.614
10.67	10	34	.576
9.98	11	35	.538
9.30	12	36	.500
8.62	13	37	.462
7.94	14	38	.424
7.26	15	39	.387
6.57	16	40	.348
5.89	17	41	.311
5.21	18	42	.273
4.53	19	43	.235
3.85	20	44	.197
3.16	21	45	.159
2.48	22	46	.121
1.80	23	47	.083

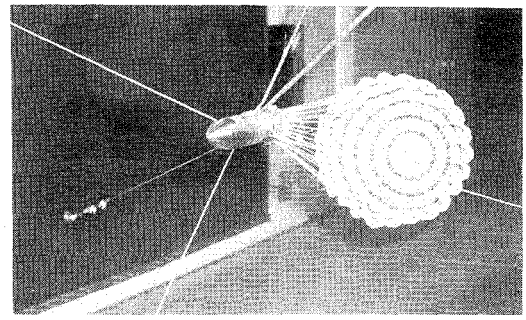

Fig. 4 Parachute model with Kulite pressure transducers.

PRESSURE PORT LOCATIONS

ORIFICE NUMBER	DISTANCE FROM VENT CENTER	ORIFICE LOCATION L/R
1	16.71	0.928
2	14.14	0.786
3	11.57	0.643
4	9.00	0.500
5	6.43	0.357
6	3.86	0.214
7	1.29	0.072

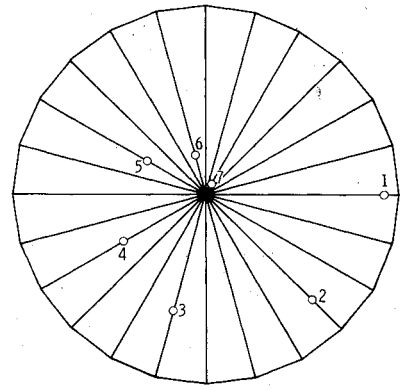

Fig. 5 Pressure port numbering system and location on canopy for dynamic opening tests.

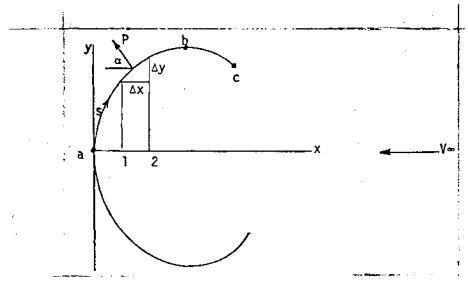

Fig. 6 Profile of canopy.

If P is assumed constant over the interval y_i to y_{i+1} Eq. (2) can be integrated to yield

$$D=\pi\sum_{i=1}^{n-1}(y_{i+1}^2-y_i^2)\overline{P_i} \tag{3}$$

where $\overline{P_i}=(P_i+P_{i+1})/2$, and n is the number of pressure ports. Now the inside pressure acts in the direction of the outer surface normal, as shown in Fig. 6, whereas the outside pressure acts in the opposite direction. Therefore the total drag is

$$D_{\text{TOTAL}}=D\,(\text{inside pressure})-D\,(\text{outside pressure}) \tag{4}$$

However, this total drag calculation assumes that the parachute canopy is solid, whereas in fact it is porous.

Table 3 Nominal test conditions

Test Facility	Dynamic Pressure Lb/ft^2	Mach no.	Reynolds Number x 10^{-6}/ft
LTV	35	0.154	1.049
LTV	50	0.184	1.254
LTV	65		
LTV	75	0.226	1.535
NSRDC	75	0.223	1.561
NSRDC	100	0.26	1.81
NSRDC	200	0.37	2.57
NSRDC	300	0.45	3.23
NSRDC	400	0.52	3.78
NSRDC	500	0.58	4.27

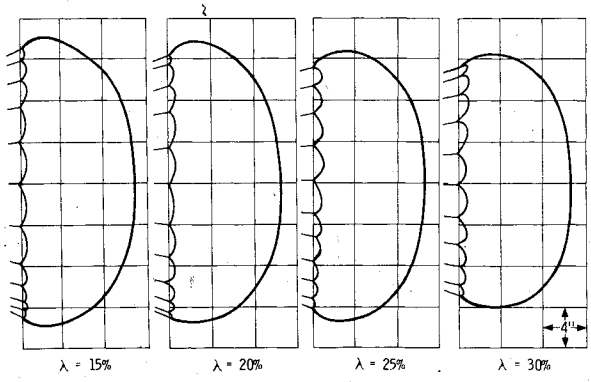

Fig. 7 Side view sketches of fully inflated parachutes ($L/D_o = 1.0$) with geometric porosities of 15, 20, 25 and 30% (LTV test).

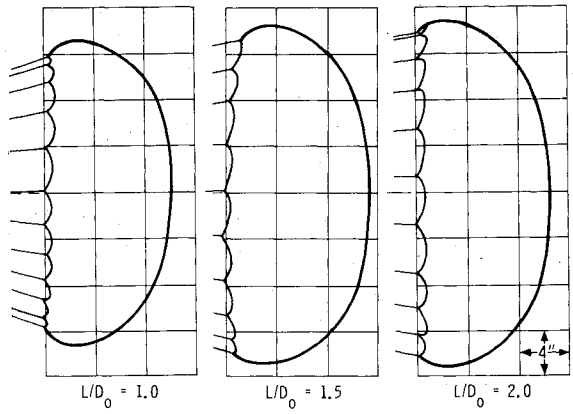

Fig. 8 Side view sketches of fully inflated parachutes with line lengths of *1.0, 1.5,* and *2.0* D_o ($\lambda = 25\%$) (LTV test).

Therefore,

$$D_{ACTUAL} = D_{TOTAL}\ (1.00 - \%\ \text{porosity}/100).$$

An additional correction was made for the drag of the suspension lines with the assumption of a form drag coefficient of 1.10 and a friction drag coefficient of 0.005. The friction drag of the suspension lines was calculated by using the component of velocity parallel to the lines. The angle between the lines and the flow direction was obtained from photographs like Fig. 3. This friction drag was very small, being about 1/3 of 1% of the measured drag force for the parachute. The suspension line form drag was calculate using the velocity component perpendicular to the suspension lines and was about 9% of the measured drag force.

The parachute shapes necessary in the above data reduction were taken from 70-mm black and white still photographs taken perpendicular to the profile of the parachute for every configuration at each dynamic pressure for which that configuration was run. These photographs were used to measure

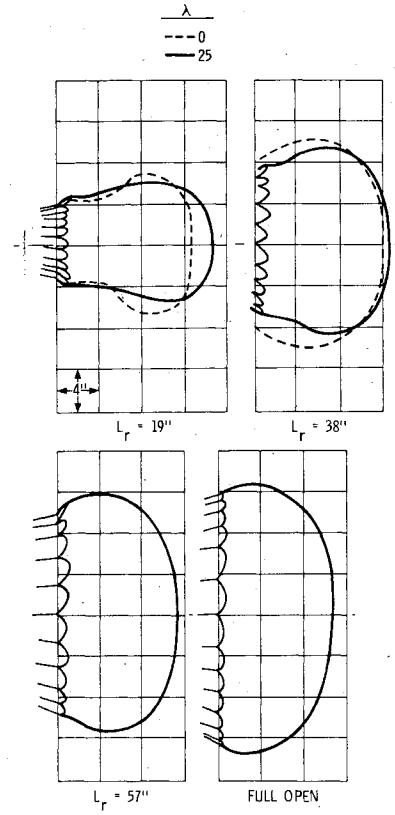

Fig. 9 Effect of reefing on canopy profile ($\lambda = 25\%$)(LTV test).

the vertical distance from the centerline to each pressure port, as required in the pressure integration described previously. The photographs also were used to measure the parachute inflated diameter.

Results

At LTV all tests were conducted with the tunnel test section vented to atmosphere. This procedure yields a static pressure approximately equal to ambient. Most of the testing at NSRDC was done using the same technique. Typical test conditions can be seen in Table 3. For the highest speed tested, the NSRDC tunnel was run with the stagnation chamber vented to get the highest possible Mach number (0.78) with the tunnel configuration being utilized.

Side view profile sketches of the fully inflated parachutes taken from photographs are shown in Fig. 7 for geometric porosities of 15, 20, 25, and 30%. It can be seen that the inflated diameter increases as the porosity decreases. Fig. 8 shows that the inflated diameter also increases as the suspension line length is lengthened from *1.0* D_o to *1.5* and *2.0* D_o. The effect of reefing line lengths of 19 in., 38 in., and 57 in. relative to full open can be seen in Fig. 9 for $\lambda = 25\%$. As a comparison, the dotted shape lines are for $\lambda = 0$ (solid cloth canopy). Measured pressure distribution from the NSRDC tests is shown in Fig. 10 for $\lambda = 15$, 20, 25, and 30% ($L = 1.0D_o$).[§] The pressure distribution inside the canopy appears to be about the same for all four porosities tested. The 15 and 20% porosity canopies have greater negative pressure on the outside as compared to the 25 and 30% porosity canopies. This plus the larger projected area (see Fig. 7) results in a higher integrated pressure drag coefficient for the less porous canopies.

Figure 11 shows the effect of increasing suspension line length to *1.5* and *2.0* D_o on the canopy pressure distribution. The inside pressure distribution is about the same for all three line lengths. The suction is less near the skirt for the shortest line length ($L/d_o = 1.0$), thus resulting in lower $\Delta P/q$. This

[§] Porosities of 0 and 10% were not tested at NSRDC because of severe dynamic instability of the fully inflated canopies.

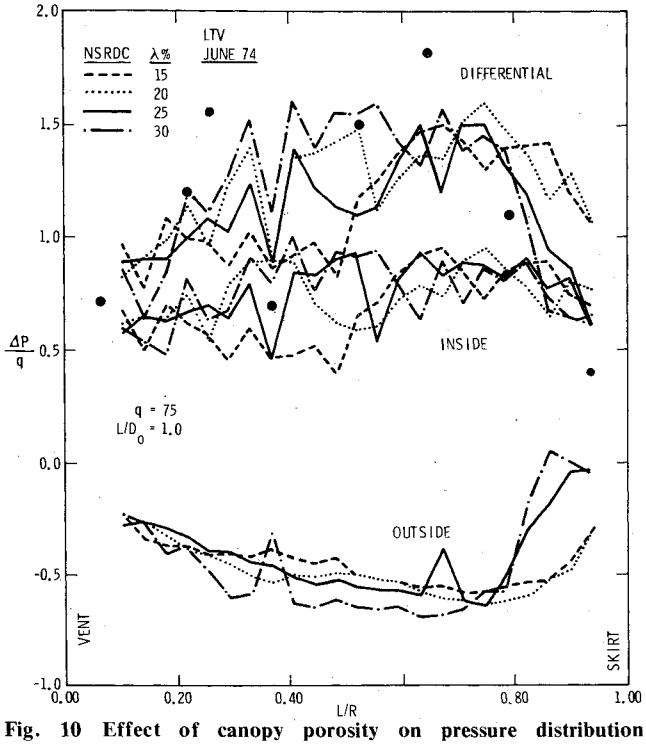

Fig. 10 Effect of canopy porosity on pressure distribution (NSRDC).

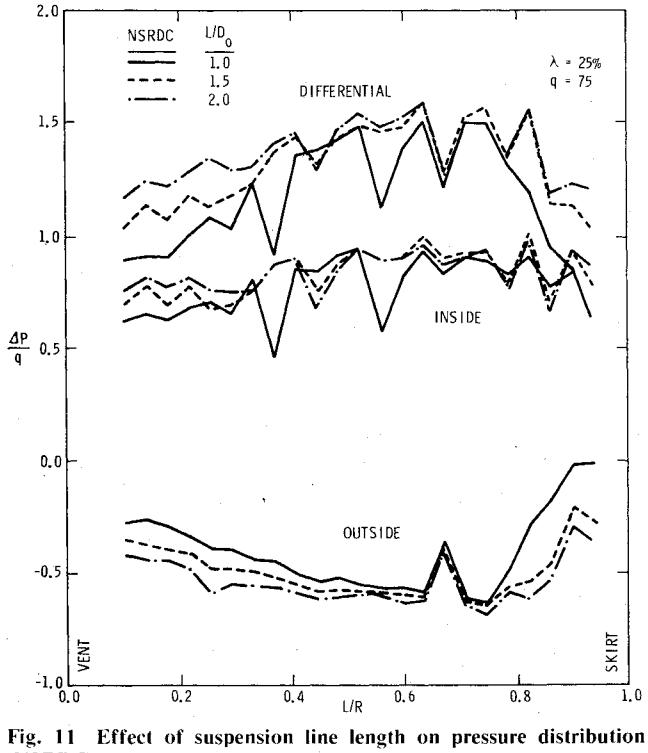

Fig. 11 Effect of suspension line length on pressure distribution (NSRDC).

effect, coupled with the smaller projected area (see Fig. 8), results in lower $C_{D_{\Delta p}}$ values for the shorter line length configurations.

The effect of reefing line lengths of 19, 38, and 57 in. on pressure distribution is shown in Fig. 12. The differential pressure drops to near zero at $L/R=0.3$ for the 19 in. long reefing line case, since the lower two-thirds of the canopy are essentially aligned with the airflow (see left side of Fig. 9).

Figure 13 shows that Mach number has very little effect on the drag coefficient as determined from integration of the pressure distributions over the canopy profiles. Figure 14 shows a comparison of drag force obtained by integration of

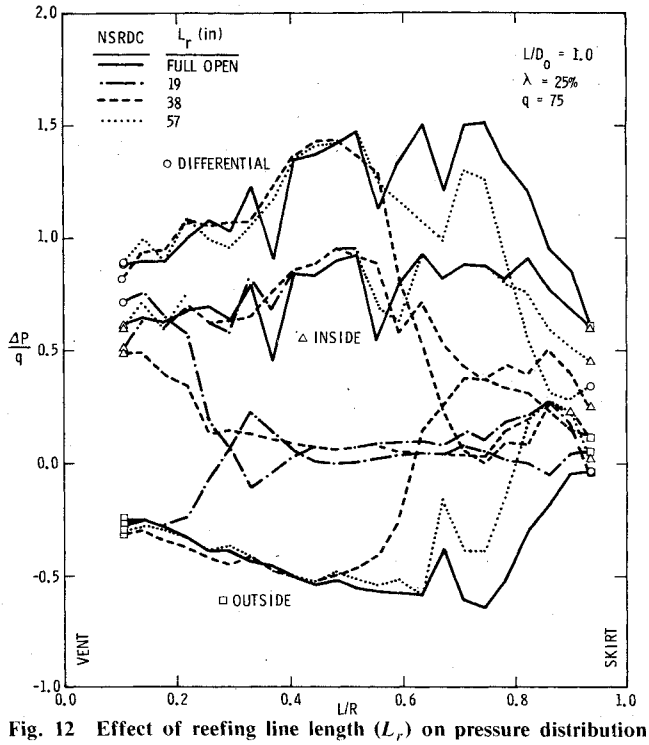

Fig. 12 Effect of reefing line length (L_r) on pressure distribution (NSRDC).

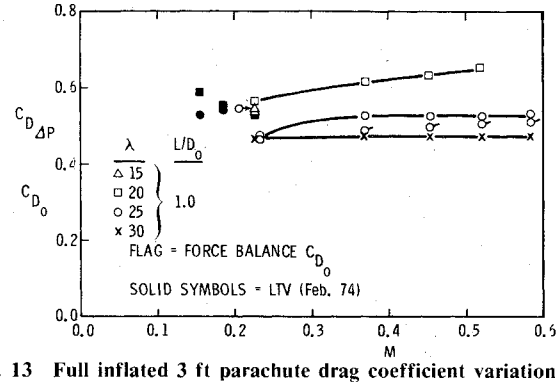

Fig. 13 Full inflated 3 ft parachute drag coefficient variation with Mach number (NSRDC, Nov. 74).

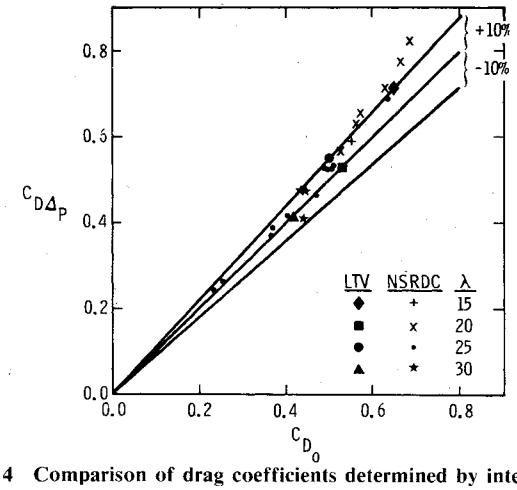

Fig. 14 Comparison of drag coefficients determined by integrating pressure distributions ($D_{d\Delta p}$) with drag balance data (D_{Do}).

the pressure distribution with drag measured by the force balance for both NSRDC and LTV tests. Agreement is generally within 10%.

The dynamic differential pressure measurements are shown in Fig. 15 during disreefing from a 25% geometric porosity

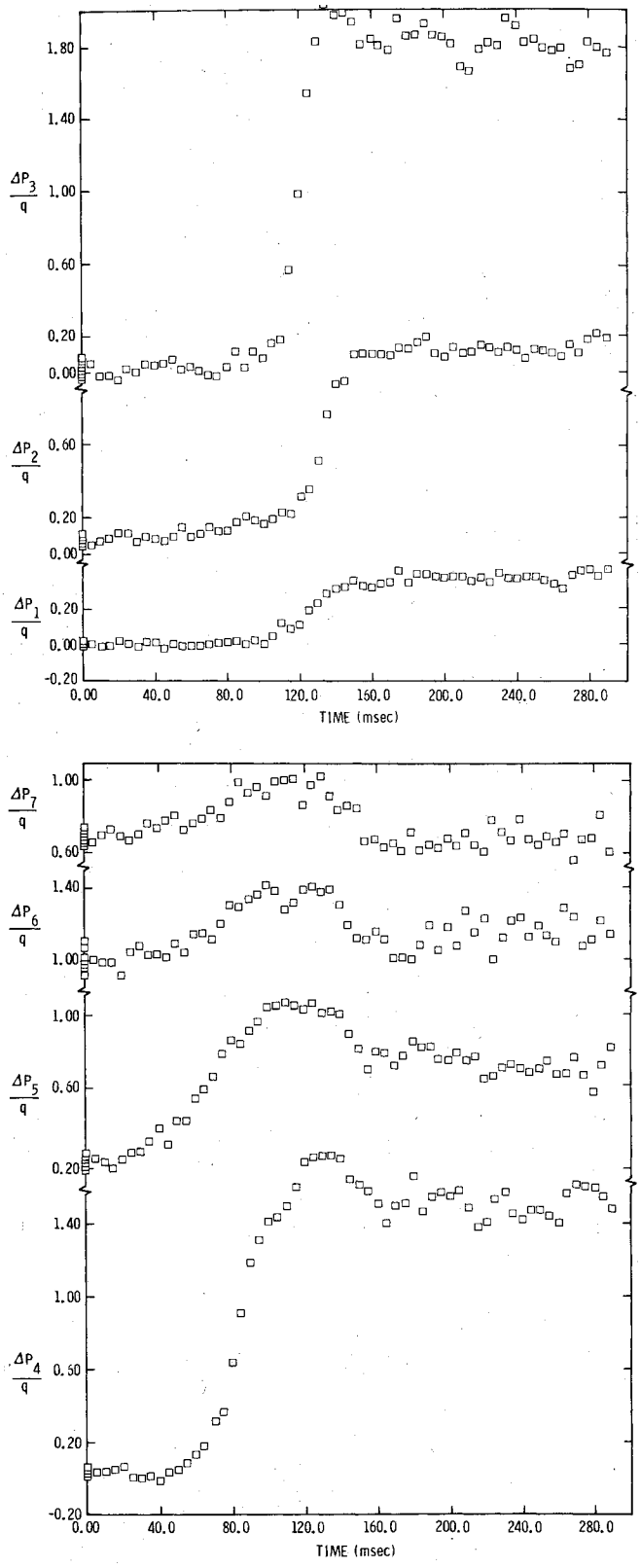

Fig. 15 Dynamic pressure data for 3 ft diameter ribbon parachute during disreefing from 19 in. reefing line length in LTV Low Speed Wind Tunnel ($q = 75$ psf).

parachute reefed with a 19 in. long reefing line. The average full-open steady-state $\Delta P/q$ values from Fig. 15 (right side of graph) are plotted as solid symbols in Fig. 10. These should be compared with the circle symbols. Agreement is good, considering the different measurement technique. The dynamic variation of the ratio of total parachute drag to dynamic pressure for the same run is shown in Fig. 16.

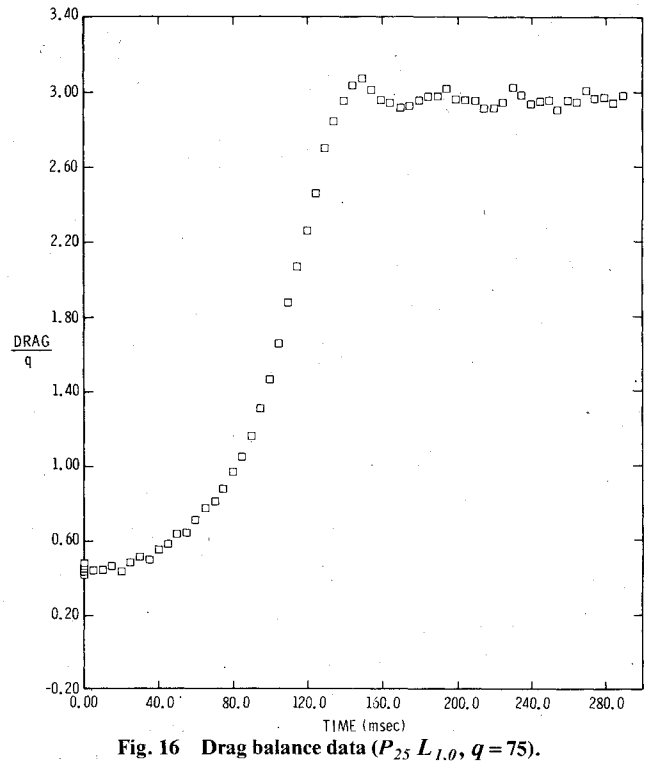

Fig. 16 Drag balance data (P_{25} $L_{1.0}$, $q = 75$).

Conclusions

The conclusions reached from studying the pressure data from wind tunnel tests of 3 ft diameter ribbon parachutes are:

1) The influence of porosity, line length, and reefing on steady-state pressure distributions is illustrated by the test data.

2) Parachute drag force obtained by integrating the measured pressure distributions over the photographically obtained canopy side profiles agreed within 10% with the drag force measured by a force balance in the test body. This tends to validate the accuracy of the data.

3) Pressure distribution data obtained from two wind tunnels are in good agreement.

4) Initial measurements of dynamic pressures obtained during disreefing are in general agreement with the steady-state data.

References

[1] Dickie, G.D., Jr., "Tests of FIST Ribbon Parachutes in the VAC 8-ft Subsonic Wind Tunnel," United Aircraft Corporation, Report No. R-1408-1, February 1959 (done on Sandia Laboratories Purchase Order 51-2203).

[2] Heinrich, H.G. and Saari, D.P., "Study of Parachute Forces and Canopy Pressure Distribution Measured in a Subsonic Wind Tunnel Under Infinite Mass Conditions," AFFDL-TR-71-175, March 1972.

[3] Heinrich, H.G., Noreen, R.A., and Dale, J.N., "Aerodynamic Coefficients and Pressure Distribution of Solid Flat and Ringslot Models in One Dimensional Velocity Gradients," AFFDL-TR-73-113, Dec. 1973.

[4] Melzig, H.D. and Schmidt, P.K., "Pressure Distribution During Parachute Opening, Phase I, Infinite Mass Opening Case," Technical Report AFFDL-TR-66-10, March 1966.

[5] Holbrook, J.W., "Sandia Corporation Pressure and Disreefing Test of Model Parachutes in the Vought Systems Division Low Speed Wind Tunnel," (done on Sandia Laboratories Purchase Order 63-2139), SAND 74-0278A, Sept. 3, 1974.

[6] Vaughn, J.B., "Sandia Corporation Pressure and Disreefing Test of Model Parachutes in the Vought Systems Division Low Speed Wind Tunnel," LSWT-455, (Sandia Laboratories Purchase Order 63-2139), SAND 74-0278A, Sept. 25, 1974.

[7] Ottensoser, Jonah, "Ribbon and Gliding Type Parachutes Evaluated in the 7 by 10 foot Transonic Wind Tunnel," April 1975, Sand 75-7072.

[8] McVey, D.F., Pepper, W.B., and Reed, J.F., "A Wind Tunnel Parametric Study of Ribbon Parachutes," AIAA Paper 75-1370, Albuquerque, N. Mex., 1975.